Atmospheric pressure atomic layer deposition for in-channel surface modification of PDMS microfluidic chips

Santoso, Albert; David, M. Kristen; Boukany, Pouyan E.; van Steijn, Volkert; van Ommen, J. Ruud

DOI
10.1016/j.cej.2024.155269

Publication date
2024

Document Version
Final published version

Published in
Chemical Engineering Journal

Chemical Engineering Journal 498 (2024) 155269

Contents lists available at ScienceDirect

Chemical Engineering Journal

journal homepage: www.elsevier.com/locate/cej

Atmospheric pressure atomic layer deposition for in-channel surface modification of PDMS microfluidic chips

Albert Santoso, M. Kristen David, Pouyan E. Boukany, Volkert van Steijn, J. Ruud van Ommen *

Department of Chemical Engineering, Delft University of Technology, van der Maasweg 9, 2629 HZ, Delft, The Netherlands

ARTICLE INFO

Keywords:
Atomic layer deposition
Microfluidics
Polydimethylsiloxane
In situ surface modification

ABSTRACT

Polydimethylsiloxane (PDMS) is one of the materials of choice for the fabrication of microfluidic chips. However, its broad application is constrained by its incompatibility with common organic solvents and the absence of surface anchoring groups for surface functionalization. Current solutions involving bulk-, ex-situ surface-, and in-situ liquid phase modifications are limited and practically demanding. In this work, we present a simple, novel strategy to deposit a metal oxide nano-layer on the inside of bonded PDMS microfluidic channels using atmospheric pressure atomic layer deposition (AP-ALD). Using three important classes of microfluidic experiments, i.e., (i) the production of micron-sized particles, (ii) the cultivation of biological cells, and (iii) the photocatalytic degradation in continuous flow chemistry, we demonstrate that the metal oxide nano-layer offers a higher resistance against organic solvent swelling, higher hydrophilicity, and a higher degree of further functionalization of the wall. We demonstrate the versatility of the approach by not only depositing SiO_x nano-layers, but also TiO_x nano-layers, which in the case of the flow chemistry experiment were further functionalized with gold nanoparticles through the use of AP-ALD. This study demonstrates AP-ALD as a tool to broaden the applicability of PDMS devices.

1. Introduction

For the past two decades, polydimethylsiloxane (PDMS) is the choice material for the development of micro analysis systems [1,2], lab-on-a-chips [3,4], micro-reactors [4,5], and organ-on-a-chips [6]. Despite the unique material properties and especially the ease of replication and rapid prototyping, bare PDMS does not resist common organic solvents, absorbs various (bio)molecules, and is difficult to functionalize robustly [7,8]. Current solutions involve bulk or surface modification of PDMS prior to bonding the microfluidic channels. Yet, doping the PDMS can reduce the optical transparency [9], while depositing a ceramic coating before bonding results in less leak-tight microchannels [10]. Hence, various methods for the in-channel modification of the surface of bonded PDMS microfluidic have been developed, to render the walls inert or provide them with the required functionality, without sacrificing the advantageous properties of PDMS [11–14].

In-channel surface modification methods can be classified into liquid [15,16] and gas phase methods [17]. Most in-channel surface modification methods make use of liquids flown through bonded microchannels to deposit either organic molecules and/or an inorganic layer [13]. However, the introduced layer may be relatively thick with respect to the dimensions of the microchannels [13,16], and conformal coating of a network of channels poses a challenge due to the entrapment of air and/or coating solution during filling and/or emptying of a channel network [18].

Gas phase methods, on the contrary, are known to be able to coat a surface with high resolution [19]. In particular, atomic layer deposition (ALD) offers exceptional conformality and tunable film composition [20,21]. By exposing the surface to alternating, self-limiting reactions, one can grow nano-layers and control the thickness at the Angstrom level [22]. These deposited nano-layers offer attractive surface functionality, for example in terms of their catalytic-, barrier-, wetting-, and other properties, interesting for many applications [20–22]. Despite the potential, to the authors' best knowledge, conventional ALD has never been used for in-channel modification of bonded PDMS microfluidic channels. Typically, ALD, like many other established gas (plasma) treatments, is carried out in a vacuum chamber with a surface directly exposed to the gases in the chamber [23]. Consequently, in-channel coating of bonded PDMS microchannels would require impractically long exposure times for the ALD precursors to react over the full length of the channels in case their transport is solely based on diffusion. The diffusion distance can however be minimized if the ALD precursors are flown through the channels. This requires a reasonable pressure drop along the microchannels, which is possible when carrying

* Corresponding author.
E-mail address: J.R.vanommen@tudelft.nl (J.R. van Ommen).

https://doi.org/10.1016/j.cej.2024.155269

Available online 30 August 2024

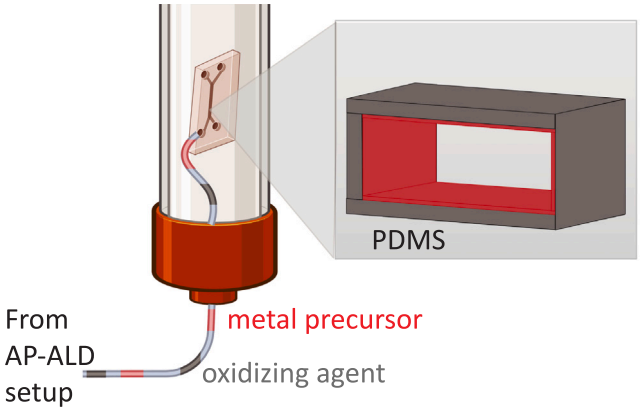

Fig. 1. Illustration of in-channel coating of bonded PDMS microfluidic chips by alternatingly flowing a metal precursor and an oxidizing agent through the channels of a microfluidic chip for the atomic layer deposition of a nano-layer of metal oxide on the inside of the microfluidic channels. For safety reasons, the microfluidic chip is placed in the tubular glass column of a home-built atmospheric pressure atomic layer deposition (AP-ALD) setup. The two metal-oxides deposited in this work to allow the use of organic solvents and the functionalization of the channel walls are silicon oxide (SiO_x) and titanium oxide (TiO_x).

out ALD at atmospheric pressure. Furthermore, in earlier work we have shown that the obtained coatings on flat PDMS surfaces are superior with AP-ALD as compared to vacuum-based ALD process [7,8]. Therefore, forcing the ALD precursors through the microchannels using convective flow offers an attractive route to address the challenge to coat long microchannels, akin to deep trenches and benefits from all advantages of gas phase ALD.

In this study, we explore the use of convective flow via atmospheric pressure ALD (AP-ALD) for in-channel functionalization of bonded PDMS microfluidic channels through a layer of metal oxide. The concept is illustrated in Fig. 1, which shows that we alternatingly flow ALD precursors through a bonded microfluidic chip, which is enclosed in a tubular glass reactor connected to a home-built AP-ALD setup. In this way, we deposit a nano-layer of metal oxide on all walls of the microfluidic channels (silicon oxide as well as titanium oxide), rendering them inert against organic solvents, and providing surface functionality in terms of their wetting and photocatalytic properties and, at the same time, rendering them inert against organic solvents. These metal oxide layers hence offer additional benefits over commonly used organic layers that effectively functionalize the surface, but do not render it inert [16,24]. We demonstrate the beneficial properties for three important classes of applications in the field of microfluidics: the production of microparticles, the cultivation of biological cells, and the photocatalytic degradation of a pollutant. The presented results show the potential use of AP-ALD to modify the walls of bonded microfluidic channels, broadening the application window of PDMS chips [14,25].

2. Experimental

2.1. Fabrication of PDMS microfluidic chips

We fabricated PDMS microfluidic chips using soft lithography. In short, a negative photoresist (SU-8 2050, micro resist technology GmbH) was spin-coated on top of a 4 inch silicon wafer following the recipe of the manufacturer before baked at 100 °C for 15 min to obtain a 50 μm thick layer. The coated wafer was then loaded onto a LaserWriter (Heidelberg, 1 μm laser beam at 365 nm), where the two-dimensional layout of the microchannels (Autocad 2019, Autodesk, see Fig. S1) was written on the wafer. After laser writing, we soft-baked the wafer at 100 °C for 5 min, developed the patterned photoresist coating using propylene glycol methyl ether acetate (PGMEA, >99.5%, Merck Sigma) for 10 min, and post-baked the thus obtained master mold at 200 °C for 30 min.

To fabricate PDMS microfluidic chips from the master mold, we mixed the elastomer and curing agent (Sylgard 184 Elastomer Kit, Dow Corning Comp.) in a mass ratio of 10:1. After degassing, we poured the mixture over the master mold placed in a 5 inch Petri dish. We cured the PDMS at 70 °C for at least 8 h. The PDMS slab was then gently removed from the wafer and cut to size. PDMS chips were obtained by punching inlets and outlets into the pieces of PDMS using a 1.5 mm biopsy puncher, washing them with ethanol to remove debris, and bonding them on glass slides spin-coated with a 20 μm thick PDMS layer (2000 rpm for 2 min, Laurell WS-650-23B) using an oxygen plasma treatment (Harrick PDC-002) at 0.2–0.4 mbar for 140 s. The bonded chips were stored in the oven at 70 °C before use.

2.2. In-channel coating of bonded microfluidic chips using AP-ALD

To coat the inner walls of the bonded PDMS microfluidic chips with a thin layer of metal oxide, we used a home-built atmospheric-pressure ALD (AP-ALD) setup with a tubular glass column. One microfluidic chip was placed inside the column and one of the inlets of the chip was directly connected to the inlet of the column through a polytetrafluorethylene (PTFE) tube (outer diameter 1.6 mm, inner diameter 0.5 mm, Diba, 008T16-050-200). In this way, the gases entering the column flowed entirely through the microchannels. The role of the column was to safely contain the excess reactants and byproducts. The metal oxide nano-layer was grown on the walls of the microchannels by subsequently flowing a metal precursor and an oxidizing agent through the chip, both in the gas phase, separated by a purge with nitrogen gas in order to remove excess reactants and byproducts. The thickness of the nano-layer was controlled by the number of such sequences, commonly referred to as ALD cycles.

The simplified process flow diagram of the setup is shown in Fig. S2. Nitrogen gas (N_2 99.999%, Linde) was used to carry the metal precursor as well as to purge the chip through the use of three gate valves, two connected to a dip-tube bubbler that contains the metal precursor, and one to the tubular glass column, as shown in Fig. S2. When the two valves connected to the dip-tube bubbler opened and the middle (by-pass) valve closed, nitrogen gas first flowed into the dip-tube bubbler, and then into the column and the microchannels. When both valves connected to the dip-tube bubbler closed, and the by-pass valve opened, nitrogen gas bypassed the dip-tube bubbler, purging the microchannels and the column. From the column, the gases flowed through a series of two trapping bottles, and subsequently through a carbon filter, before being released in a fume hood.

Two types of metal oxides were used in this work: silicon oxide and titanium oxide. All development and characterization studies were done using silicon oxide, while two complementary case studies, showing the versatility of the ALD approach, were done with titanium oxide. The deposition of the SiO_x nano-coating was conducted using silicon tetrachloride ($SiCl_4$, Alfa Aesar) as the metal precursor and ozone-treated humidified air as the oxidizing agent. The stream of the oxidizing agent was made by flowing compressed air through metallic tubing to an ozonator (Sander Certizon), and then to a dip-tube bubbler containing water at room temperature. Unless stated otherwise, the silicon precursor, kept in the bubbler at room temperature, flowed at 0.2 L/min for an exposure time of 10 s, while the oxidizing agent flowed at 0.2 L/min for an exposure time of 30 s. In between, nitrogen purging was done at 0.2 L/min for 100 s. The AP-ALD treatment was carried at 50 °C for different numbers of ALD cycles (5, 20, 50, and 100 cycles). The gas flow leaving the glass column was neutralized by flowing it through a series of two trapping bottles, both containing a solution of 10% (w/v) sodium hydroxide (Merck Sigma).

The deposition of the TiO_x nano-coating was conducted using Tetrakis-dimethylamino titanium (IV) (TDMAT, >99.99% Merck Sigma) as the metal precursor and ozone-treated air as the oxidizing agent. The stream of the oxidizing agent was made by flowing compressed

air through metallic tubing to an ozonator, and then directly into the column. The titanium precursor, kept in the bubbler covered with a heating mantle at 70 °C, flowed at 0.2 L/min for an exposure time of 10 s, while the oxidizing agent flowed at 0.2 L/min for an exposure time of 30 s. In between, nitrogen purging was done at 0.2 L/min for 100 s. The AP-ALD treatment was carried at 100 °C for different numbers of ALD cycles (3, 25, and 100 cycles). The gas flow leaving the glass column was neutralized by flowing it through a series of two trapping bottles, both containing a mineral oil (Kaydol).

To accommodate the reaction temperature, we covered the tubing with heating cables. We furthermore heated the tubular glass column with an infrared heating lamp, see Fig. S2.

2.3. Characterization of metal oxide coating on microchannel walls

To characterize the metal oxide coating deposited on the inner walls of the bonded microfluidic channels, we made a cross-sectional cut of the ALD-treated channels using a scalpel. We analyzed the channel cross sections with field emission scanning electron microscopy (FE-SEM, Hitachi Regulus SU8230, with a beam current of 1–5 μA, electron energy of 1–10 keV, and a tilt angle of 0° to 15°). The surface morphology and the surface chemical composition were studied in more detail by conducting ALD experiments with the same operation parameters on flat samples (PDMS spin-coated on a silicon wafer) as described elsewhere [8]. The surface morphology was studied using atomic force microscopy (AFM, Bruker Dimension Icon with an amplitude of 80–150 nV, a feedback gain of 0.05–0.5, and scan rates of 0.6–0.9 Hz). The surface chemical composition was measured using X-ray photoelectron spectroscopy (XPS, ThermoFisher Scientific Nexsa, equipped with a monochromatic Al Kα radiation source and a pass energy of 30 and 100 eV for the survey scan and ion-beam etching unit). Depth profiling was conducted by etching the surface using Ar^+ ions (2 keV with a raster size of 2 mm) while a flood gun was used to compensate for the positive charge. Thermo Avantage 5.913 and CASA-XPS software packages were used to post-process and deconvolute the XPS peak profile, where the spectra were charge-corrected with the adventitious carbon peak at 284.8 eV.

On top of the above characterization of the metal oxide coating obtained for a fixed set of ALD operating parameters, we studied the influence of the temperature on the surface morphology. More specifically, we obtained FE-SEM images of the cross sections of microfluidic chips treated at 30 °C, 50 °C, and 100 °C, for a fixed number of 20 ALD cycles. Given the observed differences in morphology and the differences in possible detachment of the coating from the PDMS walls under flow, we checked the attachment of the coating to the PDMS by flowing water through the treated chips at 50 μL/min for 10 min. We studied the solution collected from the outlet of the chips using inductively coupled plasma optical emission spectroscopy (ICP-OES, PerkinElmer Optima 8000), with argon gas as a carrier.

2.4. Evaluation of AP-ALD coating in microfluidic experiments

To evaluate the performance of the metal oxide coating, we conducted two studies with coated microfluidic chips: (1) a channel wall deformation study and (2) a channel wall absorption study. Bare PDMS channel walls are known to swell and deform when exposed to organic solvents as well as to absorb small hydrophobic molecules in a liquid solvent [15,16,26]. We then performed these two studies to evaluate to what extent the metal oxide coating prevents direct contact between the PDMS and the solvent, mitigating both issues.

The channel deformation study was conducted as follows. We fabricated microfluidic chips featuring a simple long straight microchannel (length: 11.6 mm, width: 500 μm, height: 50 μm), see Fig. S1(a) for the two-dimensional layout. We coated the inner walls of the chips with a SiO_x nano-layer using 5, 20, and 100 ALD cycles. To evaluate the deformation of the channel walls when flowing an organic solvent through the channel, we used a confocal laser scanning microscope (CLSM 710, AxioObserverZ.1, Fluar 2.5x/0.12, 543 nm laser source (20%) and PMT detector). To this end, rhodamine B (Merck Sigma), a known fluorescent agent, was added to the organic solvent. More specifically, we prepared a solution of 1 μM rhodamine B in chloroform (99%, Merck Sigma). We loaded the rhodamine B solution into a 5 mL syringe (Beckton-Dickinson, Discardit II) with a non-rubber plunger, connected the syringe with PTFE tubing to the inlet of the microfluidic chip, and drove the solution through the microchannel using a syringe pump (Harvard Apparatus Pump 11 Pico Elite Plus) at a flow rate of 40 μL/min, while taking confocal (z-stack) images of the channel at 10–15 different planes across the height of the channel. From these images, we reconstructed the 3-D shape of the lumen of the microchannel using Zen 3.8 software (Zeiss), normalized to its maximum intensity (1). For reference, we first performed the same type of measurements in the same channel with a solution of 1 μM rhodamine B in demi water, since no swelling of the PDMS, and hence no deformation of the channel walls is expected for water.

The wall absorption study was conducted as follows. After fabrication and coating of the chips with a nano-layer of SiO_x through 20 ALD cycles, we injected a rhodamine B solution (30 μM, in demi water) inside bare and AP-ALD-treated PDMS microfluidic chips using a 5 mL syringe mounted on a syringe pump. After filling the channels, we left the chips (with the outlets open to air) to dry for 3 days in a dark environment, where the solutions dried through the inlets and outlets. After three days, we measured the intensity of the fluorescent agent inside the walls of the PDMS using a confocal laser scanning microscope (CLSM 980, Zeiss Axio-ObserverZ.1/7) with EC Plan-Neofluar 5×/NA 0.16 and 10×/NA 0.30 air objectives, a 543 nm laser source (0.2%, emitted 565 nm), and a GaAsP-PMT detector. Background fluorescence was reduced using the Zen autofocus strategy with the best contrast method. The intensity profile was processed using Zen 3.8 software to visualize the penetration of rhodamine B into the channel walls.

An advantage of forcing the precursor through the microfluidic channels instead of letting the precursors in the ALD tubular reactor enter the microchip through the inlets and outlets by diffusion is the ability to coat long channels and even channel networks. Rather than using the long channel used to assess the deformability of the (coated) wall, we, therefore, used the channel network as shown in Fig. S1(b) to assess the coating based on the absorption of the wall. To study to what extent the walls of the channels perpendicular to the ALD precursor flow direction were exposed to the precursors and covered by a layer of SiO_x, we performed the experiment for various pulse times of the ALD precursors (1, 10, 30, and 100 s). We kept the purge time fixed to 100 s. To confirm the location of the channel wall, we additionally took brightfield images of the bare PDMS chip (EC Plan-Neofluar 5×/NA 0.16 objective and Multialkali-PMT detector).

2.5. Case study 1: microparticle production using organic solvents

A first important class of applications in the field of microfluidics is to utilize the unsurpassed control over minute amounts of fluids to produce single, double, and even higher order emulsions, foams, and particles [27,28]. Yet, the use of organic solvents, for example, necessary to produce synthetic cells through the use of lipids that are typically dissolved in chloroform, does not permit the use of PDMS chips. In this first case study, we show the ability to use ALD-coated microfluidic chips for the production of polylactic acid microparticles using chloroform as the organic solvent.

We fabricated a microfluidic chip featuring a flow-focusing junction commonly used for the generation of droplets, see the two-dimensional layout in Fig. S1(c). We coated the walls with a nano-layer of SiO_x using 20 ALD cycles. To produce polylactic acid (PLA) microparticles, a solution of 5% (w/v) poly(D,L-lactide) (PLA, 10–18 kDa, Resomer R 202H, ester terminated, Sigma Aldrich) in chloroform was injected in the chip at a flow rate of 0.5 μL/min and broken up into droplets in a solution of 1% (w/v) poly(vinyl alcohol) (99%, hydrolyzed, Merck Sigma) in MilliQ water injected at a flow rate of 40 μL/min. The formation of the PLA droplets was observed using a camera (ImagingSource

DFK33UX273, 600 frames per second) through an LWD plan phase 40X objective lens on a light microscope (Euromex Oxion Inverso PLPH). The polymerized PLA microparticles were collected at the outlet using a glass slide after 0, 1, and 3 h of continuous production. Their photos were taken using the same camera. A minimum of 100 particles was analyzed using ImageJ to determine the particle size distribution.

2.6. Case study 2: biological cell culture on PDMS walls functionalized with titanium oxide

A second important class of applications in the field of microfluidics is to utilize control over micro environments for the study of biological cells, tissue, and organoids [11]. Yet, it is well known that cells do not adhere to bare PDMS surfaces. On top, cytotoxic uncured monomers in the PDMS matrix may leach out during cell culture, compromising the cell culture [29]. In this second case study, we show the ability to use ALD-coated microfluidic chips for the culture of biological cells using titanium oxide as a nano-layer on top of the PDMS, as this metal oxide is known to promote cell adhesion [30,31].

We fabricated a microfluidic chip featuring a growth chamber, see the two-dimensional layout in Fig. S1(d). We then coated the walls with a nano-layer of TiO_x using 3 and 25 ALD cycles. Before seeding the cell (A549-Vim-RFP, from a human lung adenocarcinoma cell line, the vimentin being tagged with a red fluorescent protein), in bare and TiO_x-coated chambers, the chips were rinsed with 70% ethanol and washed three times with complete media (see details below). The cells were seeded into the microfluidic chips at a density of approximately 3.75×10^3 cells/mL and the chips were incubated at 37 °C with 5% CO_2 in a dark environment. The cells in the chips were imaged every 24 h for 72 h using a confocal laser scanning microscope (AxioObserverZ.1/7, Plan-Apochromat 10x/0.45). We obtained red fluorescent images of cells using LED-module 567 nm laser source (50%) filtered so that the excitation wavelength was at 543–568 nm, and the emission wavelength was measured at 581–679 nm, with exposure time of 150 ms and a 56 HE GFP/DsRed reflector and an Orca Flash 4.0 V2 Hamamatsu camera. To reduce the background noise, the autofocus function of the Zen 3.8 software was used. The images were analyzed using ImageJ to derive the number of cells. The cell adhesion response on the microfluidic channel surface was studied by analyzing the sphericity of the cells after 24 h of incubation. Detached cells were indicated with the sphericity and shape factor near 1 (0.99–1.00), while the adhered cells were indicated with the sphericity and shape factor less than 1 (0.00–0.98) [32]. The experiment was repeated three times in three independent microfluidic chips. A paired comparison method with the Bonferroni post-test (OriginPro 2022) at a significance level of $p = 0.05$ was used to study the statistical significance between the results.

To check the viability of the cells, we stained the cells with calcein AM (1 μM in serum-free culture media, ITK) after 72 h of incubation. Green fluorescence images were obtained using a LED-module 475 nm laser source (2%) filtered so that the excitation wavelength was at 450–490 nm and the emission wavelength was at 500–550 nm, with a 38 HE Green Fluorescent Prot reflector and an Orca Flash 4.0 V2 Hamamatsu camera.

Preparation of the cell solution used for seeding of the PDMS chips was done as follows: cells from cell line A549-Vim-RFP (generously gifted by Peter Ten Dijk, Leiden University Medical Centre) were grown on T25 flasks (Sarstedt) using a 'complete medium'. The medium consists of Dulbecco's Modified Eagle's media (DMEM, Thermofisher), supplemented with 5% of Fetal Bovine Serum (FBS, Thermofisher), and 1% of antibiotic-antimycotic (Merck Sigma). After reaching 80% confluency, the cells were detached from the flask using trypsin (0.25% EDTA, Thermo Fisher Scientific) and counted with trypan blue (Thermo Fisher Scientific) using an automated counter (TC20, Bio-rad). The obtained cell solution was then diluted using complete media to a cell concentration of 3.75×10^3 cells/mL.

To better understand the observed behavior on the titanium-oxide coated PDMS walls, we additionally characterized the surface properties (wetting and surface chemical composition) of the TiO_x nano-layer. To be able to perform water contact angle measurements, we turned to flat samples (PDMS spin-coated on a silicon wafer) and performed the AP-ALD with the same operational parameters. Both bare and AP-ALD-treated PDMS samples were kept in water and dried before the dynamic water contact angle measurements were performed using a Krüss drop shape analyzer as described elsewhere [7]. The average advancing contact angle was reported from 10 measurements via the typical uncertainty (1 s.d.). To obtain the surface chemical composition, XPS survey scans were performed on the flat samples.

2.7. Case study 3: continuous flow chemistry at PDMS walls functionalized with a titanium oxide nano-layer and gold nanoparticles

A third important class of applications in the field of microfluidics is to perform chemical reactions under continuous flow, thereby making use of the well-known advantages of microreactor technology, including the high surface-to-volume ratio, etc. [33]. While heterogeneous catalytic reactions with a catalyst coated on the wall are interesting for a wide range of applications, including electrochemical conversions, direct functionalization of bare PDMS walls is a challenge [7,13]. In this third case study, we show the ability to use ALD-coated microfluidic chips to functionalize the PDMS walls with gold nanoparticles used for the photocatalytic degradation of a pollutant in water.

We fabricated a microfluidic chip featuring the same chamber as used for the cell study, see the two-dimensional layout in Fig. S1(d). We coated the walls with a nano-layer of TiO_x using 100 ALD cycles. We then further functionalized the TiO_x nano-layer through the deposition of gold nanoparticles (AuNPs) using trimethylphosphino-trimethyl gold(III) (6-Me, prepared as described in [34]) and ozone as the ALD precursors [35]. This AP-ALD process was carried out using nitrogen as the carrier gas flowing at 0.2 L/min at 100 °C for 5 cycles, with a pulse time for the 6-Me of 10 s and for the ozonated air of 30 s, with 100 s of nitrogen purge in between. After the deposition of the gold nanoparticles, we performed 5 additional TiO_x AP-ALD cycles. As a pollutant in the photocatalytic degradation study, we use rhodamine B. We prepared an aqueous solution of rhodamine B (17 μM, or 7.2 mg/L, in demi-water) and injected it into the coated chip using a syringe pump at a wide range of flow rates leading to a wide range of residence times in the chip (0.02, 0.04, 0.1, 0.2, 0.4, 1, 2, and 4 min). The photocatalytic conversion was done by top-exposing the chip to a visible light source (Dotlux LED-Einbaupanel, 225 mm × 225 mm, 25 W, 4000 K, 2375 lm, distanced 5 cm from the top of the chip). The inlet and outlet concentrations were measured using UV–Vis NanoDrop™ 2000/2000c Spectrophotometer (wide scan reading, with wavelengths in the range 300–800 nm). For reference, the same measurements were performed in bare PDMS microchips. For each experiment, three samples were collected from the outlet and the averages are reported.

To characterize the AuNPs inside the chip, we conducted a similar deposition and cut the chip into pieces of cross-sections. The pieces were sonicated in 1 M HNO_3 solution (65%, Merck Sigma) for 15 min, before being left immersed for 48 h to dissolve the underneath TiO_x layers and disperse the AuNPs. The immersing liquid was then centrifuged (MicroCL 21/21R, Thermoscientific) at 14,800 rpm for 10 min, decanted, washed with ethanol, and transferred onto a Quantifoil copper TEM grids. Transmission electron microscopy (TEM, JEOL JEM1400) was performed with a voltage of 120 kV and the particle size was analyzed using ImageJ.

3. Result and discussion

3.1. Characterization of the metal oxide coating on the inner walls of the microchannels

Fig. 2(a) shows FE-SEM images of the cross-section of bare and AP-ALD-treated PDMS microfluidic channels. The wall of a bare PDMS channel is relatively smooth, as shown in Fig. 2(a). In comparison,

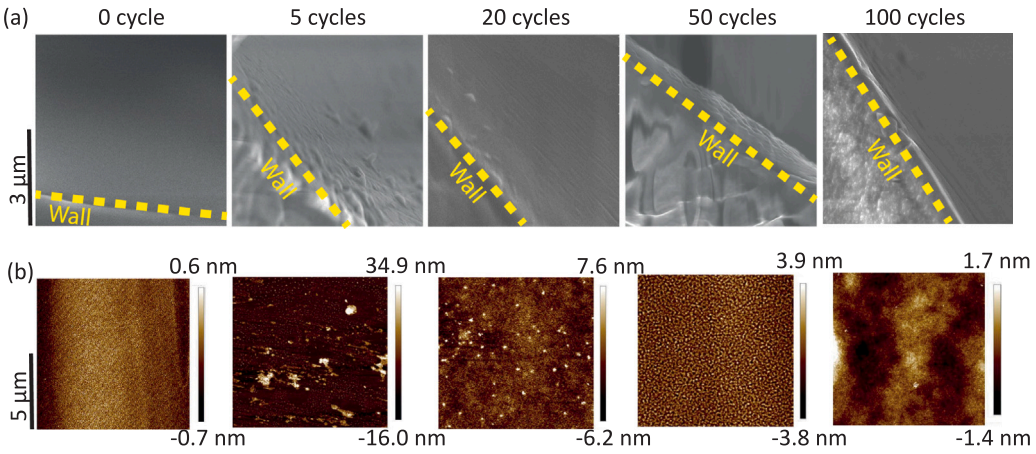

Fig. 2. (a) FE-SEM images of bare and SiO_x-coated PDMS chips obtained after making cross-sectional cuts of the chips that feature a straight 11.6 mm long, 500 µm wide, and 50 µm high microchannel. SiO_x AP-ALD treatment: 5, 20, 50, and 100 ALD cycles at 50 °C. (b) AFM surface profiles on a flat PDMS layer treated the same as in the corresponding images in (a).

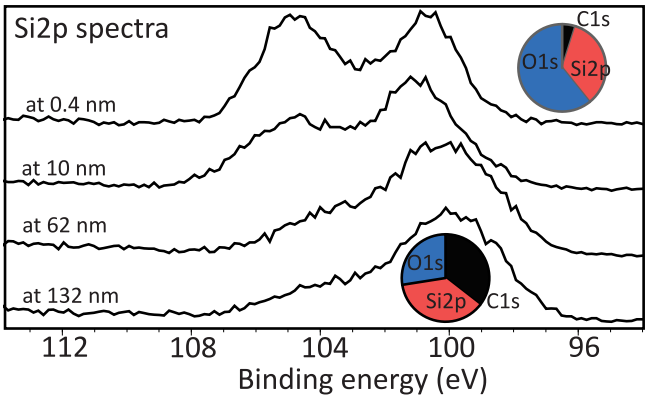

Fig. 3. Surface chemical composition of a flat PDMS layer treated with 20 ALD cycles at 50 °C (corresponding to the panels in the middle of Fig. 2) studied using XPS, showing XPS Si2p spectra obtained at different etch depths. The top graph shows the Si2p spectrum at an etch depth <1 nm and the top inset shows the corresponding atomic composition. The bottom graph shows the Si2p spectrum at an etch depth >100 nm and the bottom inset shows the corresponding atomic composition. The etch depth was approximated using the etch rate determined in our earlier work [8].

after 5 ALD cycles, patches are seen on the channel wall. These patches appear smaller in size after 20 cycles and more packed after 50 cycles. After 100 cycles, individual patches are no longer observed and the wall appears as fully covered by a sheet of SiO_x. Since the angle of the SEM beams and detectors may affect our perception of the morphology, we supplemented the surface morphology study by conducting the same depositions on a flat 20 µm thick layer of PDMS spin-coated on a silicon wafer. AFM measurements performed on bare and ALD-treated samples confirm a smooth surface for bare PDMS and a relatively rough surface after 5 ALD cycles, which gets smoother with an increasing number of ALD cycles as shown in Fig. 2(b).

In addition to the surface morphology, we characterized the chemical composition of the surface of bare and ALD-treated flat PDMS samples. Fig. 3 shows the Si2p spectra obtained at different etch depths for a PDMS sample treated with 20 ALD cycles. At the surface (depth ~0.4 nm), two peaks in the Si2p spectrum are found at 99.95 eV and 103.5 eV. When etched deeper to ~10 nm, the peak at 103.5 eV starts decreasing and the two peaks become less distinctive. At the largest etch depth of ~132 nm, we observe only one peak at 99.95 eV. While the observed peaks point to the presence of silicon, the shape and position of the peaks indicate different oxidation states of the silicon element.

To confirm the presence of a SiO_x nano-layer on the surface, we deconvolute the XPS spectra at the etch depth of ~0.4 nm. The first peak at 99.95 eV has a peak split of 0.51 eV, that easily ends up as one broad peak or an asymmetric one [36,37]. This peak, unfortunately, corresponds to all possible oxidation states of the silicon element (from Si^0 to Si^{4+}) that could be found in a silicon wafer, in a silicon oxide layer, and a PDMS sample [36,37]. However, the second peak (at 103.5 eV) corresponds exclusively to a higher Si oxidation state (e.g., Si^{3+} and Si^{4+}), typically found in a silicon oxide layer and not in a PDMS sample [38]. Therefore this peak suggests the presence of a SiO_x nano-layer at the etch depth of ~0.4 nm. We then further confirm it by conducting an XPS survey scan at a similar etch depth, shown in the corresponding pie chart (see Fig. 3, top inset). It shows that the surface is dominated by silicon and oxygen elements, with a low presence of carbon, confirming the presence of SiO_x. Of note, the low carbon presence is acceptable and can be explained by possible adventitious carbon contamination and the out-diffusion of uncured PDMS oligomers into the surface [8,39]. Looking closer at the surface composition, the atomic ratio of Si to O is found to be around 1:1.7, lower than the expected stoichiometric ratio of SiO_2. A comparable value, however, is reported by other researchers when the SiO_x is deposited at lower temperature [40], attributed to the incomplete reaction between surface-adsorbed chemical species [41].

Going deeper into the layers underneath, the decrease and shift of the distinctive peak at 103.5 eV points to the declining Si presence at a higher oxidation state (e.g. Si^{3+} and Si^{4+}). This indicates the possible formation of a mixed layer of SiO_x and PDMS, as suggested by our previous study [8]. As the layers are etched deeper (~132 nm), the disappearance of the peak at 103.5 eV suggests the absence of SiO_x. An additional XPS survey scan (see Fig. 3, bottom inset) shows the typical atomic percentage distribution of a PDMS layer as found in earlier work [8], confirming the absence of SiO_x. While the unique surface-subsurface metal oxide growth on PDMS through AP-ALD is in agreement with the reported phenomena in our previous study [8], we point out that the depth profile of the deposited layers depends on various factors, including the operating temperature [20–22].

After confirming the presence of the SiO_x nano-layer, we performed an additional study to gain insight into the effect of the AP-ALD operating temperature for a fixed number of 20 ALD cycles. When AP-ALD was carried out at 30 °C, a rugged and rough-textured surface was observed (Fig. S3(b)), that became less rough as the operating temperature increased to 50 °C (Fig. S3(c)), and even smoother at 100 °C (Fig. S3(d)). We then compared our results with the reported phenomena in the literature [42]. The rugged surface and patches obtained when we conducted the AP-ALD at lower temperatures (30 °C) are comparable with the results reported by others as they deposited

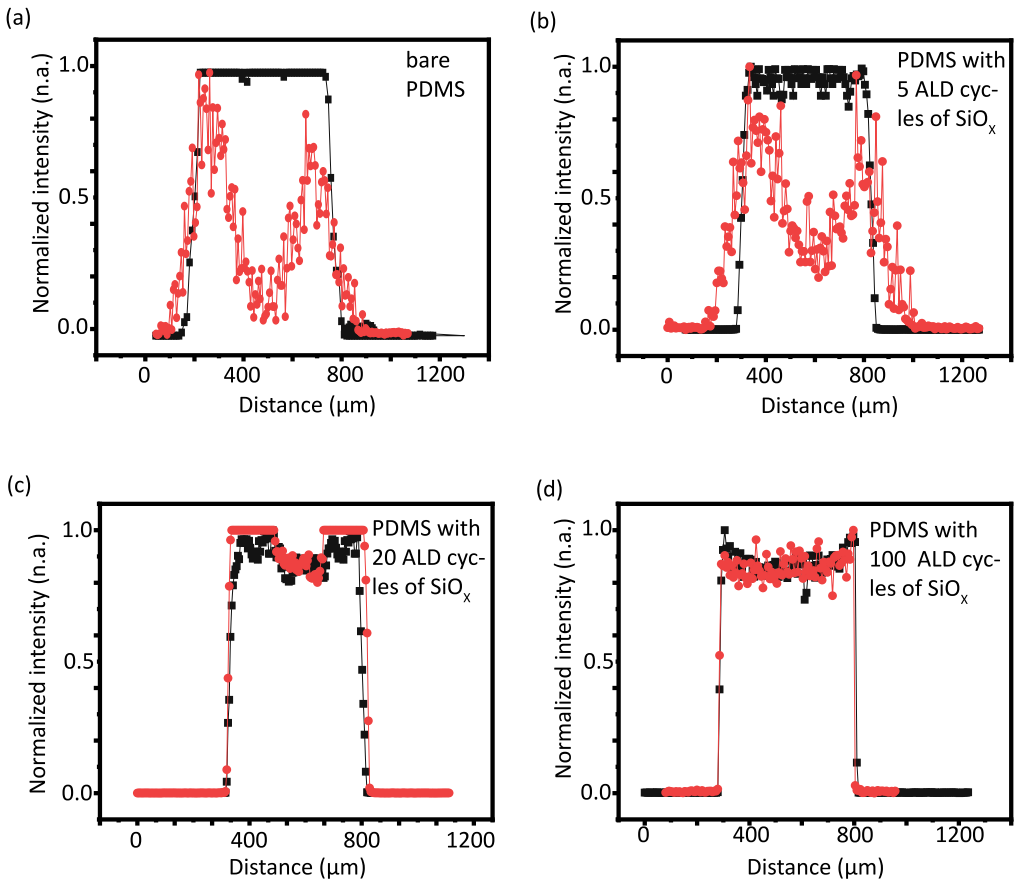

Fig. 4. Fluorescence intensity across the 500 μm wide channel, averaged of the height of 50 μm, illustrating the deformation of the cross-sectional shape of a bare PDMS chip (a) and PDMS chips treated with 5 (b), 20 (c), and 100 ALD cycles. The dark gray lines show the intensity profiles for 1 μM rhodamine B in water, while the red lines show the intensity profiles for 1 μM rhodamine B. For comparison, each intensity profile was normalized by its maximum intensity.

SiO_x at a lower temperature, without the presence of a catalyst, and on less reactive substrates [43–45]. There, they argue the presence of non-ideal ALD growth, such as condensation of ALD precursors (especially water) and hydrolysis [43,46,47], as commonly found in conventional chemical vapor deposition (CVD) of SiO_x [47]. As the operating temperature increases to 50 °C, then to 100 °C, where water molecules are expected to condense less, we obtain a smoother surface, consistent with the results reported by other groups [43].

Given that the observed differences in morphology may have an impact on how strongly the patches or layer is bound to the PDMS surface under flow, we flowed water into the channels treated with different AP-ALD operating temperatures at a relatively high flow rate (50 μL/min) for 10 min. We measured the silicon concentration in the solution collected at the channel outlet. The ICP-OES result shows that silicon (20.15 ± 0.20 mg/L) is detected for the liquid flowing in the microfluidic channel coated at 30 °C, indicating the expected weak physical bond between the deposited silicon oxide and PDMS channel wall, and indirectly corroborates the dominance of condensation (physisorption) during the deposition process. Conversely, no silicon is detected when flowing water through untreated channels and channels treated at 50 °C and 100 °C (0.10 mg/L and 0.06 mg/L respectively, lower than the reliable ICP-OES detection limit), indicating a strong bond between the metal oxide layer and the PDMS wall.

3.2. Evaluation of metal oxide coating performance in microchannel experiments

Bare PDMS microfluidic channels are known to be compatible with aqueous solutions such as water. However, when exposed to common organic solvents, PDMS swells, such that the channel walls deform and the lumen of the microchannels gets (partly) occluded [8,24]. We, therefore, evaluated to what degree the metal oxide nano-layer prevents direct contact between PDMS and the organic solvent by visualizing the extent to which the cross-section of untreated and treated microchannels deforms when flowing chloroform through the channels. We hereby note that the relatively thin layer of metal oxide provides optical access to the treated channels such that they can be studied using optical microscopy as commonly done in the field. We use the deformation study to get an indication of the coverage of the nano-layers inside the chips, given that measuring the coverage directly inside the chips is a challenging task due to uneven morphology and the non-conductive nature of PDMS channels.

In the untreated (bare) PDMS chip, a serious channel deformation is seen, as evident from the intensity profile in Fig. 4(a), where the low intensities in the middle of the 500 μm wide channel indicate that the top wall of the channel almost collapsed onto the bottom wall. The intensity of the red line increases first and declines later, indicating a larger, deformed base of the channel. While deformations are seen along the length of the channel, we note that the exact shape differs from place to place. We further note that the experiments with untreated PDMS devices are cumbersome, as some chips leaked when the chloroform solution was introduced into the channels. As expected, no deformation is observed for reference measurements with water, as evident from the well-defined, intensity profile, resembling the rectangular-shaped cross-section.

For the microchannels treated with 5 ALD cycles, we also observe channel deformation, albeit less pronounced compared to the untreated channel, see Fig. 4(b). This indicates that 5 ALD cycles result in a non-conformal coverage of the PDMS. The observation is in agreement with the previous characterization in Fig. 2, where after 5 cycles, the

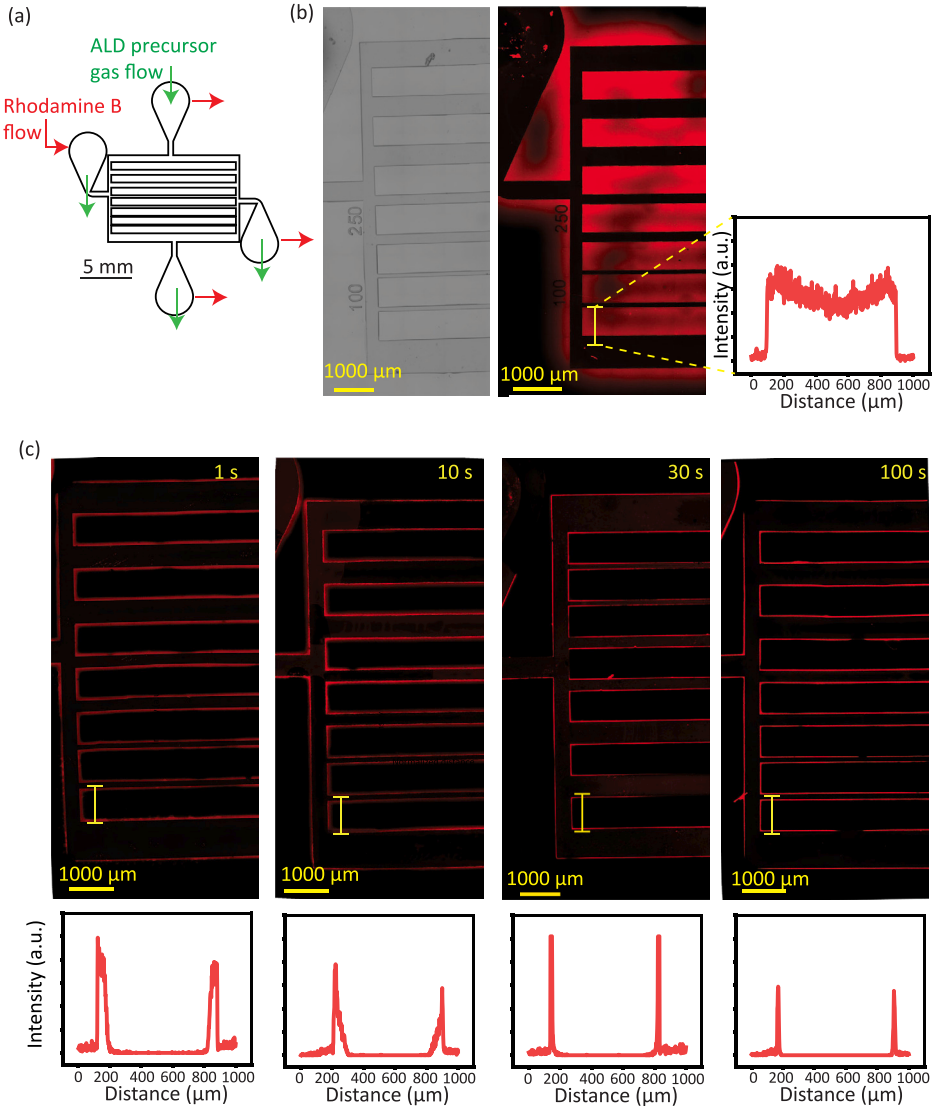

Fig. 5. (a) Microfluidic channel network featuring channels of various widths (100, 250, and 500 µm) perpendicular to the direction of flow of the ALD precursors, to visualize how far inwards these channels can be coated. The green arrows indicate the flow direction of ALD gas precursors during AP-ALD, while the red arrows show the flow of the rhodamine B solution during the wall absorption study. (b) Brightfield image of a bare PDMS microfluidic chip and fluorescence image showing the absorption of rhodamine B into the PDMS walls. (c) Fluorescence images of PDMS microfluidic chips exposed to the ALD precursors for different pulse exposure times of 1 s, 10 s, 30 s and 100 s, with the intensity profiles taken along the yellow line in the corresponding images at the bottom. SiO_x AP-ALD treatment: 20 ALD cycles at 50 °C.

PDMS surface is covered only with patches of SiO_x. On the contrary, for the microchannels treated with 20 and 100 ALD cycles, we observe overlapping intensity profiles for chloroform and water (no significant difference, as determined through a paired t-test, showing a *p*-value larger than 0.05), see Figs. 4(c) and 4(d), indicating complete SiO_x coverage of the PDMS channel walls even after repeated usage. The SiO_x layer hence prevents direct contact between PDMS and the organic solvent, demonstrating AP-ALD as a suitable approach to expand the use of PDMS microfluidic devices from aqueous solutions to organic solutions as well.

A strength of the developed approach in which ALD precursors are alternating flown through the microfluidic device is the ability to coat long microchannels as well as complete networks of microchannels. To study over what extent channels perpendicular to the direction of the flow of the ALD precursors can be coated, we treated the channel network illustrated in Fig. 5(a). The ALD precursors were flown into the chip using the inlet at the top, while the three outlets were open. We visualized the coating coverage along the channel by conducting a wall absorption study. To this end, we exposed the channels to a rhodamine B in water solution, introduced at the inlet on the left in order to fill all channels without the entrapment of air. When the PDMS microfluidic channel walls are not covered by SiO_x nano-layers, rhodamine B molecules are expected to penetrate slowly into the PDMS matrix [16,26]. Contrarily, when SiO_x nano-layers are present, the rhodamine B molecules are expected to be retained in the solution [15,16], which over the course of the experiment evaporates from the chip, leaving the rhodamine B concentrate near one of the outlets.

As expected, the fluorescent signal of rhodamine B is observed inside the walls of the untreated PDMS microfluidic chip, extending up to millimeter into the walls, see Fig. 5(b), in line with earlier work [16,26]. In contrast, the rhodamine B molecules are relatively retained at the walls in the AP-ALD-treated microfluidic channels, see Fig. 5(c). This retainment is shown over the length of the 20 mm long channel. A closer look at the fluorescence intensity near the walls shows that the fluorescent signal is found only at the edge of the walls, which drops to a non-detectable level inside the walls, see Fig. 5(c). For the shortest ALD pulse exposure time of 1 s, this drop occurs over a distance of 120 µm into the wall. For an ALD pulse exposure time of 10 s, the penetration distance into the walls is reduced, while the chips treated with pulse exposure times of 30 s and 100 s show comparable behavior

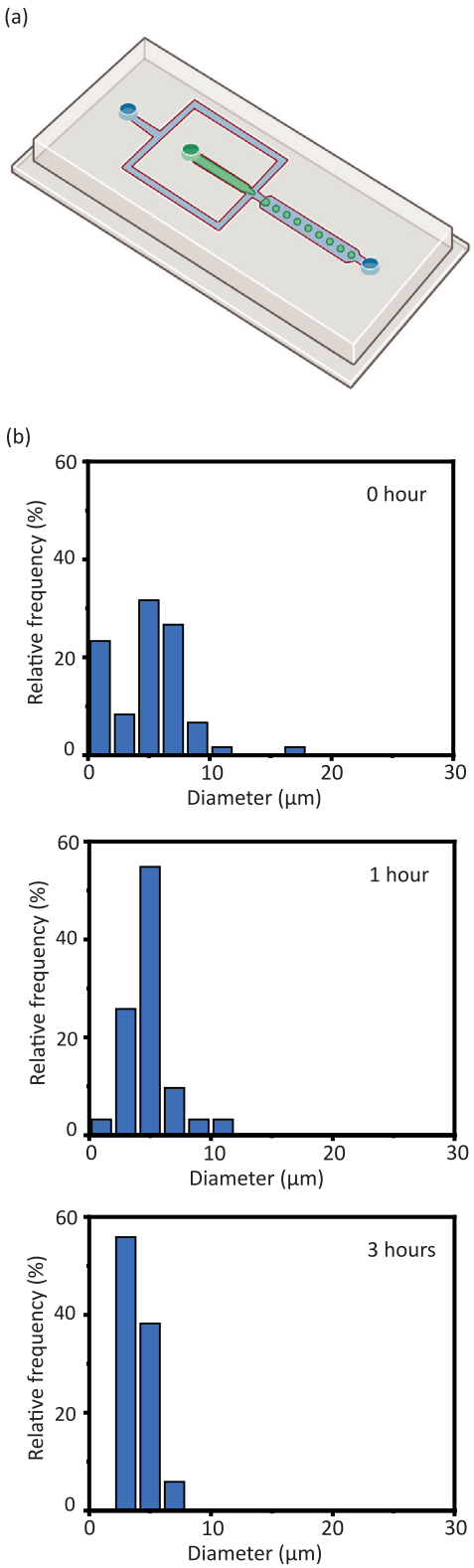

Fig. 6. (a) Illustration of the microfluidic chip featuring a 25 μm wide flow focusing junction as used for the continuous production of polylactic acid (PLA) microparticles using chloroform as an organic solvent for the PLA. (b) Distribution of the diameter of the microparticles collected off chip after 0, 1, and 3 h of continuous operations. A minimum of 100 particles was analyzed.

with minimal penetration of rhodamine B into the wall. We note that the saturation conditions in a PDMS chip are difficult to determine due to differences in the channel width (distance for the ALD precursors to reach the channel wall) and the simultaneous surface-subsurface growth occurring on PDMS. While this study shows a possible effect of a very short pulse exposure time (e.g. way lower than 1 s), it also indicates the dependence of the conformality of the coating on the flow rate. Therefore, the conformality is limited by the pressure drop achievable in the microchannel. Furthermore, this study also proves the presence of SiO_x nano-layers inside the microfluidic channels, as the nano-layers have 2–3 orders of magnitude lower relative permeability against hydrophobic molecules than bare PDMS [8], offering a barrier against rhodamine B.

3.3. Case study 1: microparticle production using organic solvents

In the first case study, we demonstrate the use of ALD-coated microfluidic chips for the production of particles using chloroform as one of the solvents. Using the chip with a flow-focusing junction illustrated in Fig. 6(a), a stream of 5% PLA in chloroform is broken up into droplets by a stream of 1% PVA in water. A few minutes after the start of the flows, a significant spread is observed in the diameter of the polymerized particles collected at the outlet, see the top panel in Fig. 6(b). More specifically, the average diameter of the particles is 4.85 μm and the coefficient of variation (CoV) is 0.63. We attribute the relatively large CoV to the formation of satellite droplets as well as to the coalescence of droplets during the stabilization of the flow. After 1 h of production, the average diameter of the droplets is about the same, 4.99 μm, and the CoV has reduced to 0.35. After 3 h of production, the average diameter is 4.98 μm and the CoV has further reduced to 0.21. For reference, we attempted to perform the same experiments in bare PDMS chips. Upon introducing chloroform in bare chips, we observe swelling of channels and narrowing of the junction, in cases followed by leakage near the inlets due to the build-up of pressure in the chips. These experiments confirm the importance of the SiO_x coating. While further optimization of the experiments to produce particles with narrower particle size distribution is certainly possible, we conclude the discussion on the case study by emphasizing a second possible advantage of the SiO_x coating, next to mitigating the problem of swelling of the PDMS. PDMS is hydrophobic in nature, which generally limits the production of emulsions in uncoated PDMS chips to water-in-oil emulsions. The SiO_x coating renders the PDMS walls hydrophilic, providing a route to produce oil-in-water emulsions.

3.4. Case study 2: biological cell culture on PDMS walls functionalized with titanium oxide

In the second case study, we demonstrate the use of ALD-coated microfluidic chips for the cultivation of biological cells at functionalized PDMS walls, hereby using TiO_x instead of SiO_x in order to illustrate the versatility of the AP-ALD approach. We functionalized the walls of a microfluidic chip featuring a circular 10 mm wide and 50 μm high chamber, see Figs. 7(a) and S1(d) and seeded epithelial, non-migratory, lung adenocarcinoma cells in the chamber. We measured the number of cells per square millimeter adhering to the bottom wall of the chamber after 24 h of incubation in bare PDMS chips and chips treated with 3 and 25 ALD cycles. The cell density is significantly higher in the AP-ALD-treated PDMS chips, as evident from Fig. 7(b) and Table 1. Especially the density of cells with a sphericity less than one, a proxy for the ease with which the cells adhere to a surface, is significantly higher in treated PDMS chips. In bare PDMS chips, ~62% of the cells are observed with sphericity less than 1, comparable to reported values in literature [32]. In treated PDMS chips, this percentage is significantly larger, i.e., ~91% and ~80% for 3 and 25 ALD cycles, respectively. This observation is in line with the notion that a more hydrophilic surface generally offers a better adherence for cells [32]. The treated surfaces are indeed considerably more hydrophilic, see Fig. S4(a), consistent with our previous work [8]. While the surface chemical composition of the chips treated with 3 and 25 cycles is slightly different (Fig. S4(b)),

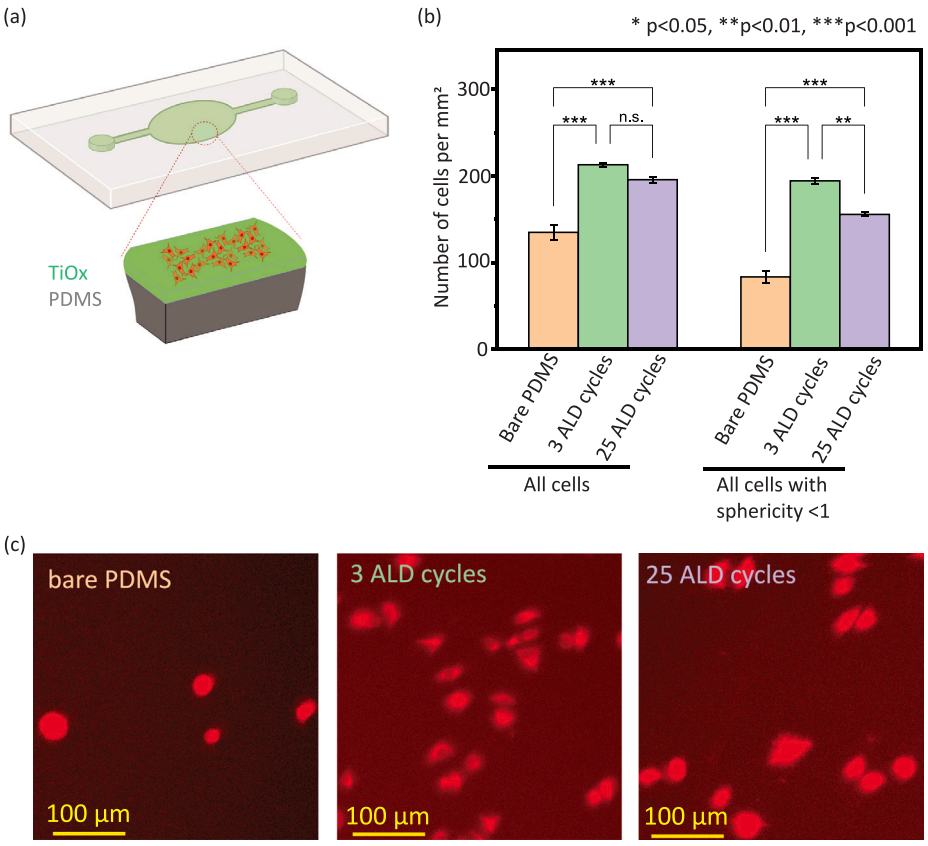

Fig. 7. (a) Illustration of the microfluidic chip featuring a circular chamber (10 mm wide and 50 µm high) as used for the case study of the attachment of cells to the walls of bare and TiO_x-coated PDMS walls. (b) Number of A549 cells per mm^2 measured after 24 h of on-chip incubation, including the number of cells with a sphericity of less than 1. Values are presented as mean ± standard error (n=3) and the corresponding numbers are provided in Table 1. (c) Representative images of cells attached to bare and TiO_x-coated PDMS walls taken after 24 h of on-chip incubation.

Table 1
Number of cells per mm^2 and the number of cells per mm^2 with sphericity less than 1 in bare and TiO_x-coated PDMS chips, measured 24 h (day 1) after incubation. Values are given as mean ± standard error (n=3).

Sample	Number of cells per mm^2	Number of cells per mm^2 with sphericity <1
Bare PDMS	135 ± 9	84 ± 7
3 ALD cycles	213 ± 3	194 ± 4
25 ALD cycles	196 ± 4	156 ± 2

Table 2
Number of cells per mm^2 in bare and TiO_x-coated PDMS chips, measured 24 h (day 1), 48 h (day 2), and 72 h (day 3) after incubation (n=3). Values are given as mean ± standard error (n=3).

Sample	Incubation time	Number of cells per mm^2
Bare PDMS	day 1	135 ± 9
	day 2	151 ± 17
	day 3	184 ± 5
3 ALD cycles	day 1	213 ± 3
	day 2	232 ± 4
	day 3	266 ± 18
25 ALD cycles	day 1	196 ± 4
	day 2	224 ± 17
	day 3	247 ± 26

we attribute the larger percentage for 3 cycles to its rougher surface [7], which is known to promote cell adhesion [48].

To study the viability of the cells, we extended the culture up to 72 h. The cell density steadily increased as shown in Fig. S4(c) and Table 2. On top, we performed a live-dead assay with calcein AM after 72 h of culture, confirming a viability of nearly ~100% in all experiments. We additionally tested the adherence of the cells after 72 h of culture, by flowing culture media inside the chips at flow rates of 0, 1, 5, 20, and 50 mL/min, confirming no meaningful differences were observed in cell density during this test, indicating strong adherence of the cells inside both the bare and treated PDMS microfluidic chips. While this case study oriented on the cultivation of cells highlights the ability to functionalize PDMS walls with a metal oxide nano-layer, the next case study highlights the ability to use the metal oxide nano-layer as a base to further functionalize the walls.

3.5. Case study 3: continuous flow chemistry at PDMS walls functionalized with a titanium oxide nano-layer and gold nanoparticles

In the third case study, we demonstrate the use of ALD-coated microfluidic chips for the photocatalytic degradation of rhodamine B dye at TiO_x-coated PDMS walls further functionalized with gold nanoparticles. Gold nanoparticles in conjunction with titanium oxide have been shown to have an increased photocatalytic activity towards various reactions, including oxidation of organic compounds [35,49]. This is explained by an enhanced absorption in the visible range due to plasmon resonance [35]. Previously, we showed that TiO_x nano-layers and AuNPs can be deposited on PDMS substrates, allowing the PDMS surface to be functionalized robustly [7]. We functionalized the walls of a microfluidic chip featuring a circular 10 mm wide and 50 µm high chamber, see Figs. 8(a) and S1(d). We flowed a rhodamine B in water solution through the chip, while exposing the chip to visible light. Fig. 8(b) shows the concentration of rhodamine B measured at the outlet of the chip relative to the initial concentration. For the shortest residence times, little to no degradation of rhodamine B is observed. As the residence time increases, the rhodamine B concentration at

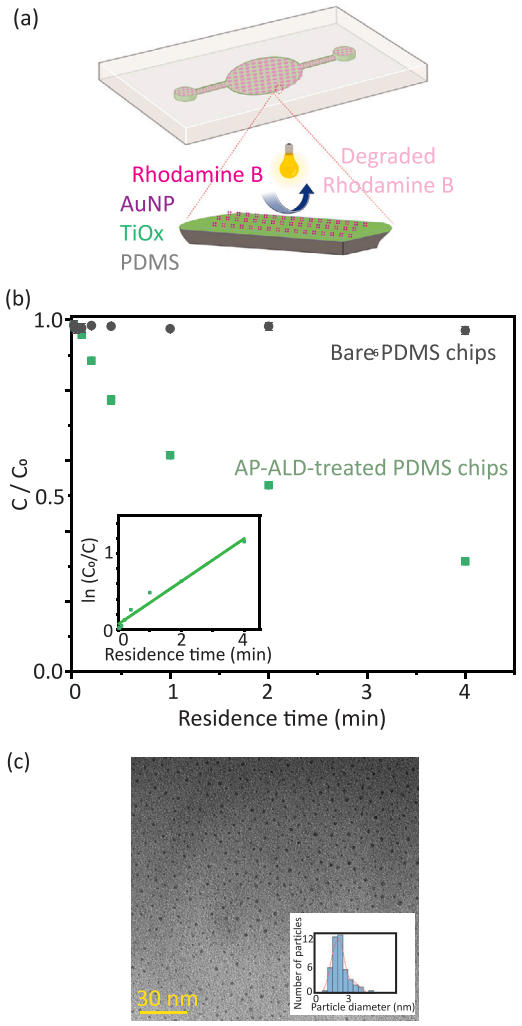

Fig. 8. (a) Illustration of the microfluidic chip featuring a circular chamber (10 mm wide and 50 μm high) as used for the case study of the photocatalytic degradation of rhodamine B at TiO_x-coated PDMS walls further functionalized with gold nanoparticles. (b) Concentration of rhodamine B at the outlet of bare and ALD-treated chips relative to the initial concentration. The inset shows a linear fit to $\ln C_0/C$ of the ALD-treated chips over the residence time. (c) TEM image of gold nanoparticles and their corresponding particle size distribution.

the outlet decreases, indicating photocatalytic reduction. The kinetics hereof is known to depend on the properties of the titanium oxide and gold nanoparticle coating [35]. The TEM indicated an average AuNP size of ~2.7 nm (Fig. 8(c)). To compare the results with earlier work, we determine an apparent kinetic constant of 0.29 min^{-1} based on the logarithmic representation of the data in the inset of Fig. 8(b), which is of the same order of magnitude as previously reported kinetic constants [35,50–52]. For reference, we performed the same experiment in a bare PDMS microfluidic chip. We observed the concentration of rhodamine B at the outlet to be comparable to the initial concentration, irrespective of the residence time, indicating no photocatalytic reaction takes place without functionalizing the PDMS walls with a TiO_x-AuNP nano-layer. While these three case studies demonstrate the benefit of the deposited nano-layers inside the channel, the approach can be extended to other metal oxides (e.g. AlO_x, ZnO_x, PtO_x, IrO_x, AgO_x), other metals (e.g. platinum, iridium, silver), or even other metal forms (sulfides, nitrides). The introduced layers can also be functionalized with other groups, such as functionalizing metal oxide with amine-containing groups [53,54], functionalizing AuNPs with thiol-containing groups [55], or using them in combination with other gas processing [56]. This versatility, along with the possible scalability due to cost reduction from the absence of low-pressure (vacuum) technologies/auxiliaries needed to operate the processes, makes AP-ALD an attractive process to coat bonded microfluidic chips.

4. Conclusion

In conclusion, we find that AP-ALD is useful for modifying the surface of bonded PDMS microfluidic channels in a simple and controlled manner. By depositing various metal oxide nano-layers, i.e., SiO_x and TiO_x, two weak points of PDMS are simultaneously solved: the weak resistance against common organic solvents and the lack of surface anchoring groups for surface functionalization. After studying how the morphology of the metal oxide nano-layers depends on important ALD operating parameters such as the temperature and the number of cycles we alternatingly flow a metal precursor followed by an oxidizing agent, we illustrate the use of the coated PDMS microfluidic devices in three classes of microfluidic applications. The developed approach for the in-channel treatment enables various applications, that are otherwise unattainable with untreated PDMS chips.

CRediT authorship contribution statement

Albert Santoso: Writing – original draft, Visualization, Methodology, Investigation, Formal analysis, Data curation, Conceptualization. **M. Kristen David:** Writing – original draft, Validation, Methodology, Investigation, Formal analysis, Conceptualization. **Pouyan E. Boukany:** Writing – review & editing, Investigation, Formal analysis, Data curation, Conceptualization. **Volkert van Steijn:** Writing – review & editing, Supervision, Project administration, Conceptualization. **J. Ruud van Ommen:** Writing – review & editing, Supervision, Project administration, Conceptualization.

Declaration of competing interest

The authors declare that they have no known competing financial interests or personal relationships that could have appeared to influence the work reported in this paper.

Data availability

Data will be made available on request.

Acknowledgments

This publication is part of the Open Technology Programme (with project number 16913) financed by the Dutch Research Council (NWO), The Netherlands. We thank Mojgan Talebi, Cas Veenhoven, Duco Bosma, Hozanna Miro and Stefan ten Hagen for their technical support during the ALD experiments. We also thank Eden Goodwin and Sean Barry for the synthesis of the ALD gold precursor. We furthermore thank Jan-Willem Hurkmans for fruitful discussions and extend our gratitude to Runjie Zheng and Nick Wijers. We acknowledge the use of Biorender in making some figures.

We extend our heartfelt gratitude to Professor Guy Marin for his leadership in the field of Chemical Reaction Engineering over the past several decades. Under his guidance, significant advancements have been made in research, including CO_2 utilization and the tailoring of catalysts through atomic layer deposition. Beyond his research contributions, Professor Marin has played numerous pivotal roles within the community. He has chaired evaluation panels and served as an editor for the Chemical Engineering Journal, among other positions. We are deeply appreciative of the exemplary standard he has set for the community.

Supplemental information

The supplemental information consists of Figs. S1 to S4 and Tables 1 and 2.

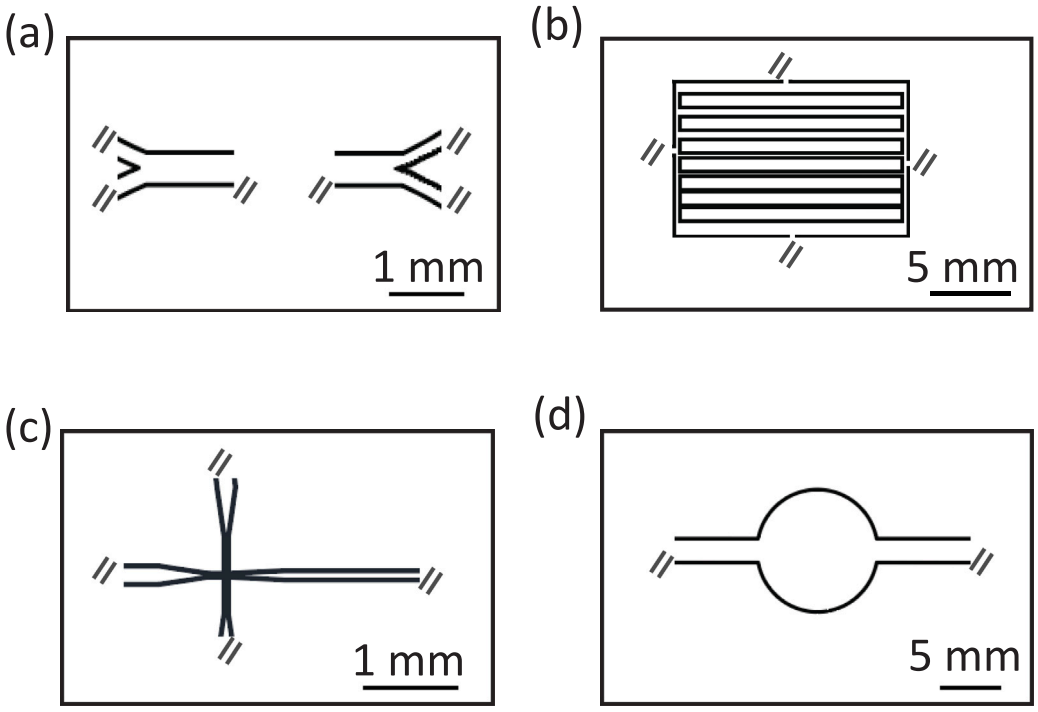

Fig. S1. Two-dimensional layouts of the microfluidics chips used in this work: (a) Y-Y junction chip used in the characterization study (Sections 2.3 and 2.4), (b) pillar chip used in the study of coating coverage (Section 2.4), (c) flow focus junction chip used in the case study of PLA microparticles production (Section 2.5), and (d) chamber chip used in the case study of A549 cells' interaction with nano-layers (Section 2.6) and in the case study of photocatalytic reduction of water pollutant model (Section 2.7). The height of the channels of all chips produced by printing these two-dimensional layouts onto a layer of photoresists is determined by the thickness of the photoresist layer, which was 50 μm. The inlets and outlets of the chips are not shown.

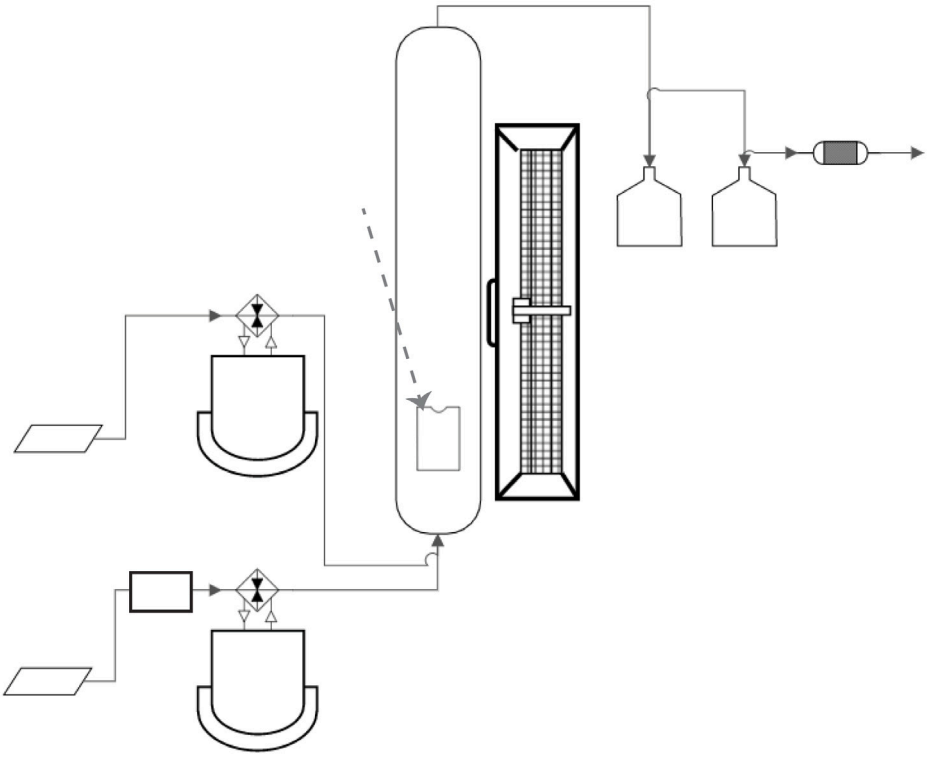

Fig. S2. Simplified process flow diagram of the home-built atmospheric-pressure ALD (AP-ALD) setup.

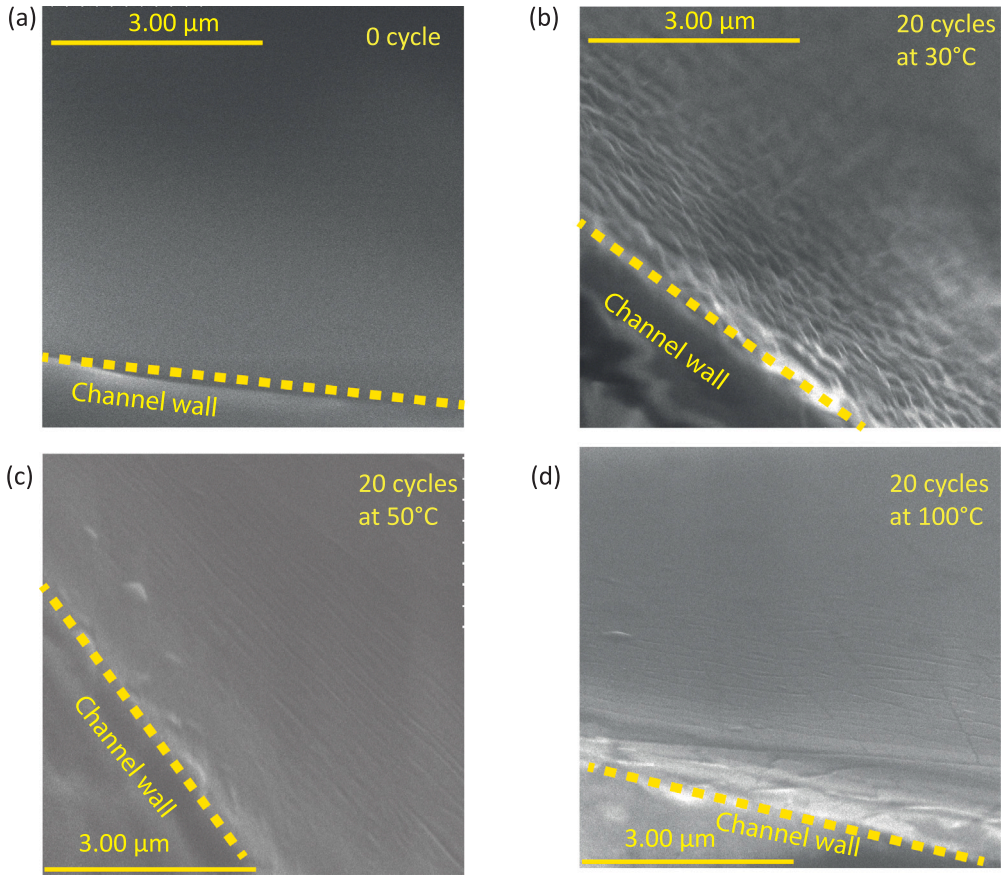

Fig. S3. FE-SEM images of bare and SiO_x-coated PDMS chips obtained after making cross-sectional cuts of the chips that feature a straight 11.6 mm long, 500 µm wide, and 50 µm high microchannel. SiO_x AP-ALD treatment: 20 ALD cycles at 30 °C, 50 °C, and 100 °C.

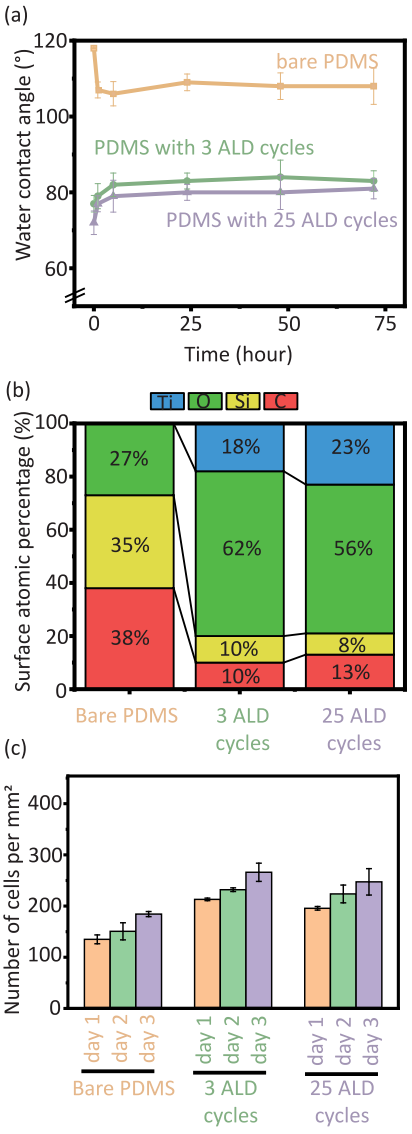

Fig. S4. (a–b) Characterization of the surface properties of the TiO_x nano-layer on flat samples, with the advancing water contact angle in (a) and the surface chemical composition in (b). (c) Density of the cells grown on bare and AP-ALD-treated PDMS microfluidic chambers for 24 to 72 h. TiO_x AP-ALD treatment: 3 and 25 ALD cycles at 100 °C.

References

[1] W.-R. Shin, G. Ahn, J.-P. Lee, I.-H. Oh, J.-Y. Ahn, Y.-H. Kim, S. Chae, Recent advances in engineering aptamer-based sensing and recovery of heavy metals and rare earth elements for environmental sustainability, Chem. Eng. J. (2023) 144742.

[2] N. Chu, Q. Liang, W. Hao, Y. Jiang, P. Liang, R.J. Zeng, Microbial electrochemical sensor for water biotoxicity monitoring, Chem. Eng. J. 404 (2021) 127053.

[3] H. Shi, K. Nie, B. Dong, M. Long, H. Xu, Z. Liu, Recent progress of microfluidic reactors for biomedical applications, Chem. Eng. J. 361 (2019) 635–650.

[4] P. Martinez-Bulit, A. Sorrenti, D.R. San Miguel, M. Mattera, Y. Belce, Y. Xia, S. Ma, M.-H. Huang, S. Pané, J. Puigmartí-Luis, In flow-based technologies: A new paradigm for the synthesis and processing of covalent-organic frameworks, Chem. Eng. J. 435 (2022) 135117.

[5] C.-Y. Lee, W.-T. Wang, C.-C. Liu, L.-M. Fu, Passive mixers in microfluidic systems: A review, Chem. Eng. J. 288 (2016) 146–160.

[6] Q. Wu, J. Liu, X. Wang, L. Feng, J. Wu, X. Zhu, W. Wen, X. Gong, Organ-on-a-chip: Recent breakthroughs and future prospects, Biomed. Eng. Online 19 (2020) 1–19.

[7] A. Santoso, B.J. van den Berg, S. Saedy, E. Goodwin, V. van Steijn, J.R. van Ommen, Robust surface functionalization of PDMS through atmospheric pressure atomic layer deposition, Atom. Layer Depos. 1 (2023) 1–13.

[8] A. Santoso, A. Damen, J.R. van Ommen, V. van Steijn, Atmospheric pressure atomic layer deposition to increase organic solvent resistance of PDMS, Chem. Commun. 58 (77) (2022) 10805–10808.

[9] J. Liu, Y. Yao, X. Li, Z. Zhang, Fabrication of advanced polydimethylsiloxane-based functional materials: Bulk modifications and surface functionalizations, Chem. Eng. J. 408 (2021) 127262.

[10] M.A. Eddings, M.A. Johnson, B.K. Gale, Determining the optimal PDMS–PDMS bonding technique for microfluidic devices, J. Micromech. Microeng. 18 (6) (2008) 067001.

[11] S. Torino, B. Corrado, M. Iodice, G. Coppola, PDMS-based microfluidic devices for cell culture, Inventions 3 (3) (2018) 65.

[12] A.-G. Niculescu, C. Chircov, A.C. Bîrcă, A.M. Grumezescu, Fabrication and applications of microfluidic devices: A review, Int. J. Mol. Sci. 22 (4) (2021) 2011.

[13] A. Shakeri, S. Khan, T.F. Didar, Conventional and emerging strategies for the fabrication and functionalization of PDMS-based microfluidic devices, Lab Chip 21 (16) (2021) 3053–3075.

[14] D. Cambie, C. Bottecchia, N.J. Straathof, V. Hessel, T. Noel, Applications of continuous-flow photochemistry in organic synthesis, material science, and water treatment, Chem. Rev. 116 (17) (2016) 10276–10341.

[15] G.T. Roman, C.T. Culbertson, Surface engineering of poly (dimethylsiloxane) microfluidic devices using transition metal sol–gel chemistry, Langmuir 22 (9) (2006) 4445–4451.

[16] A.R. Abate, D. Lee, T. Do, C. Holtze, D.A. Weitz, Glass coating for PDMS microfluidic channels by sol–gel methods, Lab Chip 8 (4) (2008) 516–518.

[17] J. Zhou, A.V. Ellis, N.H. Voelcker, Recent developments in PDMS surface modification for microfluidic devices, Electrophoresis 31 (1) (2010) 2–16.

[18] H. Becker, C. Gärtner, Polymer microfabrication technologies for microfluidic systems, Anal. Bioanal. Chem. 390 (1) (2008) 89–111.

[19] H.-Y. Chen, Y. Elkasabi, J. Lahann, Surface modification of confined microgeometries via vapor-deposited polymer coatings, J. Am. Chem. Soc. 128 (1) (2006) 374–380.

[20] R.W. Johnson, A. Hultqvist, S.F. Bent, A brief review of atomic layer deposition: from fundamentals to applications, Mater. Today 17 (5) (2014) 236–246.

[21] H. Van Bui, F. Grillo, J.R. van Ommen, Atomic and molecular layer deposition: off the beaten track, Chem. Commun. 53 (1) (2017) 45–71.

[22] J.R. van Ommen, A. Goulas, R.L. Puurunen, Atomic layer deposition, in: Kirk-Othmer Encyclopedia of Chemical Technology, John Wiley & Sons, Ltd, ISBN: 9780471238966, 2021, pp. 1–42.

[23] J. Yim, E. Verkama, J.A. Velasco, K. Arts, R.L. Puurunen, Conformality of atomic layer deposition in microchannels: impact of process parameters on the simulated thickness profile, Phys. Chem. Chem. Phys. 24 (15) (2022) 8645–8660.

[24] R. Geczy, D. Sticker, N. Bovet, U.O. Häfeli, J.P. Kutter, Chloroform compatible, thiol-ene based replica molded micro chemical devices as an alternative to glass microfluidic chips, Lab Chip 19 (5) (2019) 798–806.

[25] K.S. Elvira, R.C. Wootton, A.J. deMello, et al., The past, present and potential for microfluidic reactor technology in chemical synthesis, Nature Chem. 5 (11) (2013) 905–915.

[26] M.A. Iyer, D. Eddington, Storing and releasing rhodamine as a model hydrophobic compound in polydimethylsiloxane microfluidic devices, Lab Chip 19 (4) (2019) 574–579.

[27] L. Chen, C. Yang, Y. Xiao, X. Yan, L. Hu, M. Eggersdorfer, D. Chen, D. Weitz, F. Ye, Millifluidics, microfluidics, and nanofluidics: manipulating fluids at varying length scales, Mater. Today Nano 16 (2021) 100136.

[28] R. Geczy, M. Agnoletti, M.F. Hansen, J.P. Kutter, K. Saatchi, U.O. Häfeli, Microfluidic approaches for the production of monodisperse, superparamagnetic microspheres in the low micrometer size range, J. Magn. Magn. Mater. 471 (2019) 286–293.

[29] K.J. Regehr, M. Domenech, J.T. Koepsel, K.C. Carver, S.J. Ellison-Zelski, W.L. Murphy, L.A. Schuler, E.T. Alarid, D.J. Beebe, Biological implications of polydimethylsiloxane-based microfluidic cell culture, Lab Chip 9 (15) (2009) 2132–2139.

[30] M. Motola, J. Capek, R. Zazpe, J. Bacova, L. Hromadko, L. Bruckova, S. Ng, J. Handl, Z. Spotz, P. Knotek, K. Baishya, P. Majtnerova, J. Prikryl, H. Sopha, T. Rousar, J.M. Macak, Thin TiO_2 coatings by ALD enhance the cell growth on TiO_2 nanotubular and flat substrates, ACS Appl. Bio Mater. 3 (9) (2020) 6447–6456.

[31] J. Capek, M. Sepúlveda, J. Bacova, J. Rodriguez-Pereira, R. Zazpe, V. Cicmancova, P. Nyvltova, J. Handl, P. Knotek, K. Baishya, H. Sopha, L. Smid, T. Rousar, J.M. Macak, Ultrathin TiO_2 coatings via atomic layer deposition strongly improve cellular interactions on planar and nanotubular biomedical Ti substrates, ACS Appl. Mater. Interfaces (2024).

[32] A. Zuchowska, P. Kwiatkowski, E. Jastrzebska, M. Chudy, A. Dybko, Z. Brzozka, Adhesion of MRC-5 and A549 cells on poly (dimethylsiloxane) surface modified by proteins, Electrophoresis 37 (3) (2016) 536–544.

[33] A. Günther, K.F. Jensen, Multiphase microfluidics: from flow characteristics to chemical and materials synthesis, Lab Chip 6 (12) (2006) 1487–1503.

[34] M.B. Griffiths, P.J. Pallister, D.J. Mandia, S.T. Barry, Atomic layer deposition of gold metal, Chem. Mater. 28 (1) (2016) 44–46.

[35] F.S. Hashemi, F. Grillo, V.R. Ravikumar, D. Benz, A. Shekhar, M.B. Griffiths, S.T. Barry, J.R. van Ommen, Thermal atomic layer deposition of gold nanoparticles: controlled growth and size selection for photocatalysis, Nanoscale 12 (16) (2020) 9005–9013.
[36] G. Beamson, High-resolution XPS of organic polymers, The Scienta ESCA 300 Database (1992).
[37] P. Louette, F. Bodino, J.-J. Pireaux, Poly (dimethyl siloxane) (PDMS) XPS reference core level and energy loss spectra, Surf. Sci. Spectra 12 (1) (2005) 38–43.
[38] D. Mitchell, K. Clark, J. Bardwell, W. Lennard, G. Massoumi, I. Mitchell, Film thickness measurements of SiO_2 by XPS, Surf. Interface Anal. 21 (1) (1994) 44–50.
[39] B. Gong, J.C. Spagnola, G.N. Parsons, Hydrophilic mechanical buffer layers and stable hydrophilic finishes on polydimethylsiloxane using combined sequential vapor infiltration and atomic/molecular layer deposition, J. Vacuum Sci. Technol. A 30 (1) (2012) 01A156.
[40] T. Nam, H. Lee, T. Choi, S. Seo, C.M. Yoon, Y. Choi, H. Jeong, H.K. Lingam, V.R. Chitturi, A. Korolev, et al., Low-temperature, high-growth-rate ALD of SiO_2 using aminodisilane precursor, Appl. Surf. Sci. 485 (2019) 381–390.
[41] G. Dingemans, C. Van Helvoirt, D. Pierreux, W. Keuning, W. Kessels, Plasma-assisted ALD for the conformal deposition of SiO_2: process, material and electronic properties, J. Electrochem. Soc. 159 (3) (2012) H277.
[42] J.W. Klaus, O. Sneh, S.M. George, Growth of SiO_2 at room temperature with the use of catalyzed sequential half-reactions, Science 278 (5345) (1997) 1934–1936.
[43] D. Arl, V. Rogé, N. Adjeroud, B. Pistillo, M. Sarr, N. Bahlawane, D. Lenoble, SiO_2 thin film growth through a pure atomic layer deposition technique at room temperature, RSC Adv. 10 (31) (2020) 18073–18081.
[44] G.-Y. Fang, L.-N. Xu, Y.-Q. Cao, L.-G. Wang, D. Wu, A.-D. Li, Self-catalysis by aminosilanes and strong surface oxidation by O_2 plasma in plasma-enhanced atomic layer deposition of high-quality SiO_2, Chem. Commun. 51 (7) (2015) 1341–1344.
[45] M. Putkonen, M. Bosund, O.M. Ylivaara, R.L. Puurunen, L. Kilpi, H. Ronkainen, S. Sintonen, S. Ali, H. Lipsanen, X. Liu, et al., Thermal and plasma enhanced atomic layer deposition of SiO_2 using commercial silicon precursors, Thin Solid Films 558 (2014) 93–98.
[46] N.E. Richey, C. De Paula, S.F. Bent, Understanding chemical and physical mechanisms in atomic layer deposition, J. Chem. Phys. 152 (4) (2020) 040902.
[47] G. Fang, L. Xu, J. Ma, A. Li, Theoretical understanding of the reaction mechanism of SiO_2 atomic layer deposition, Chem. Mater. 28 (5) (2016) 1247–1255.
[48] M. Nouri-Goushki, L. Angeloni, K. Modaresifar, M. Minneboo, P.E. Boukany, M.J. Mirzaali, M.K. Ghatkesar, L.E. Fratila-Apachitei, A.A. Zadpoor, 3D-printed sub-micron patterns reveal the interrelation between cell adhesion, cell mechanics, and osteogenesis, ACS Appl. Mater. Interfaces 13 (29) (2021) 33767–33781.
[49] Z. Long, Q. Li, T. Wei, G. Zhang, Z. Ren, Historical development and prospects of photocatalysts for pollutant removal in water, J. Hazard. Mater. 395 (2020) 122599.
[50] A.-L. Liu, Z.-Q. Li, Z.-Q. Wu, X.-H. Xia, Study on the photocatalytic reaction kinetics in a TiO_2 nanoparticles coated microreactor integrated microfluidics device, Talanta 182 (2018) 544–548.
[51] S. Witzel, A.S.K. Hashmi, J. Xie, Light in gold catalysis, Chem. Rev. 121 (14) (2021) 8868–8925.
[52] S.Y. Lee, D. Kang, S. Jeong, H.T. Do, J.H. Kim, Photocatalytic degradation of rhodamine b dye by TiO_2 and gold nanoparticles supported on a floating porous polydimethylsiloxane sponge under ultraviolet and visible light irradiation, ACS Omega 5 (8) (2020) 4233–4241.
[53] D. Meroni, L. Lo Presti, G. Di Liberto, M. Ceotto, R.G. Acres, K.C. Prince, R. Bellani, G. Soliveri, S. Ardizzone, A close look at the structure of the TiO_2-APTES interface in hybrid nanomaterials and its degradation pathway: an experimental and theoretical study, J. Phys. Chem. C 121 (1) (2017) 430–440.
[54] M. Hu, S. Noda, T. Okubo, Y. Yamaguchi, H. Komiyama, Structure and morphology of self-assembled 3-mercaptopropyltrimethoxysilane layers on silicon oxide, Appl. Surf. Sci. 181 (3–4) (2001) 307–316.
[55] P.D. Jadzinsky, G. Calero, C.J. Ackerson, D.A. Bushnell, R.D. Kornberg, Structure of a thiol monolayer-protected gold nanoparticle at 1.1 A resolution, Science 318 (5849) (2007) 430–433.
[56] D. La Zara, F. Zhang, F. Sun, M.R. Bailey, M.J. Quayle, G. Petersson, S. Folestad, J.R. van Ommen, Drug powders with tunable wettability by atomic and molecular layer deposition: From highly hydrophilic to superhydrophobic, Appl. Mater. Today 22 (2021) 100945.